© 2016. Published by The Company of Biologists Ltd | Journal of Experimental Biology (2016) 219, 1187-1202 doi:10.1242/jeb.135657

RESEARCH ARTICLE

Forces generated during stretch in the heart of the lobster *Homarus americanus* are anisotropic and are altered by neuromodulators

E. S. Dickinson, A. S. Johnson*, O. Ellers and P. S. Dickinson

ABSTRACT

Mechanical and neurophysiological anisotropies mediate three-dimensional responses of the heart of *Homarus americanus*. Although hearts *in vivo* are loaded multi-axially by pressure, studies of invertebrate cardiac function typically use uniaxial tests. To generate whole-heart length–tension curves, stretch pyramids at constant lengthening and shortening rates were imposed uniaxially and biaxially along longitudinal and transverse axes of the beating whole heart. To determine whether neuropeptides that are known to modulate cardiac activity in *H. americanus* affect the active or passive components of these length–tension curves, we also performed these tests in the presence of SGRNFLRFamide (SGRN) and GYSNRNYLRFamide (GYS). In uniaxial and biaxial tests, both passive and active forces increased with stretch along both measurement axes. The increase in passive forces was anisotropic, with greater increases along the longitudinal axis. Passive forces showed hysteresis and active forces were higher during lengthening than shortening phases of the stretch pyramid. Active forces at a given length were increased by both neuropeptides. To exert these effects, neuropeptides might have acted indirectly on the muscle via their effects on the cardiac ganglion, directly on the neuromuscular junction, or directly on the muscles. Because increases in response to stretch were also seen in stimulated motor nerve-muscle preparations, at least some of the effects of the peptides are likely peripheral. Taken together, these findings suggest that flexibility in rhythmic cardiac contractions results from the amplified effects of neuropeptides interacting with the length–tension characteristics of the heart.

KEY WORDS: Neuromechanics, Biomechanics, Cardiac ganglion, Length–tension curve, Stretch feedback

INTRODUCTION

Crustacean hearts can provide a model for understanding the neuromechanics of heart function because the heart in the crustacean open circulatory system exhibits the same primary phases of the cardiac cycle as does the heart in the mammalian closed circulatory systems: isovolumetric contraction, ventricular emptying, isovolumetric relaxation and ventricular filling (e.g. in shrimp hearts, Guadagnoli et al., 2007). Furthermore, in terms of passive mechanical properties, both vertebrate hearts (Demer and Yin, 1983) and crustacean hearts (Meyhöfer, 1993) have viscoelastic material properties that are important to the function of the heart.

Biology Department, Bowdoin College, 6500 College Station, Brunswick, ME 04011, USA.

*Author for correspondence (ajohnson@bowdoin.edu)

Received 8 December 2015; Accepted 5 February 2016

The biophysical characteristics of both invertebrate and vertebrate cardiac muscle have been described by length–tension curves (Hibberd and Jewell, 1982; Demer and Yin, 1983; Meyhöfer, 1993; Linke et al., 1994). Individual cardiac fibers in the crab *Cancer magister* exhibit a non-linear increase in passive force across the physiological range of sarcomere length (Meyhöfer, 1993), as do vertebrate cardiac myocytes. In vertebrates, passive stiffness is lower at a given sarcomere length in skeletal myocytes than it is in cardiac myocytes (Granzier and Irving, 1995). This altered passive stiffness in cardiac passive tension resists the filling of the heart and may help maintain the physiological sarcomere length in the ascending limb of the length–tension curve.

Passive tension is important in the Frank–Starling effect, in which the contraction force of the heart muscle increases with stretch throughout its operating range. Resting length is at or near the start of the ascending limb. This contrasts with length–tension curves of skeletal muscle, in which the largest contraction force typically occurs in the middle of the operating range of muscle lengths (Allen and Kentish, 1985; Burkholder and Lieber, 2001). Vertebrate cardiac length–tension curves have several potential mechanisms by which the ascending limb is effectively extended, for instance by length-dependent changes in calcium sensitivity (de Tombe et al., 2010). These mechanisms generate a length–tension curve that effectively has only increasing tension, or only modest decreases in force at longer sarcomere lengths. A match of length–tension curves and stroke length ensures the Frank–Starling imperative of a continuously increasing contractile force with increasing stretch in some vertebrate hearts. For example, fish and amphibians, which tend to vary stroke volume more than mammals, have correspondingly longer sarcomere lengths at which peak active forces occur (Shiels and White, 2008).

The extent to which the Frank–Starling law applies to the lobster cardiac system is presently unknown. In fact, the myocardial length–tension curve of the American lobster, *Homarus americanus*, has not been characterized. The only reported length–tension curve is from the ostial muscle, where the passive force increased linearly with stretch and the active force was much less than the passive force (Yazawa et al., 1999). Given the different functions of ostial and other cardiac muscles and the anatomical similarities between crab hearts (Meyhöfer, 1993) and lobster hearts (Alexandrowicz, 1932), the passive length–tension curve for the lobster heart could closely resemble that of crab cardiac muscle: a nonlinear increase in passive force at greater extensions.

The range of orientations of the muscle fibers of the heart complicates the understanding of muscle length–tension curves in the context of whole hearts. Because hearts are naturally loaded three-dimensionally via pressure, the forces generated and resisted by the heart arise from the passive and active components of force acting across many axes. Thus, as the heart contracts and stretches,

Journal of Experimental Biology (2016) 219, 1187-1202 doi:10.1242/jeb.135657

List of symbols and abbreviations

CG	cardiac ganglion
CPG	central pattern generator
f	force (in grams)
GYS	GYSNRNYLRFamide
h	initial length of cylinder
L_o	original (baseline) length, before application of stretch pyramids
r	radius of cylinder
r_f	final radius after contraction
r_i	initial radius before contraction
SRGN	SGRNFLRFamide
v	initial volume of cylinder
x	extension (in mm)
ΔF	change in force from L_o to ΔL_{max}
ΔF_{active}	change in active force
$\Delta F_{passive}$	change in passive force
ΔF_{total}	change in total force
Δh	initial – final cylinder length
ΔL	change in length
ΔL_{max}	maximum change in length
$\Delta \dot{L}$	extension rate
Δr	initial – final radius
Δv_l	initial – final cylinder volume due to length change
Δv_r	initial – final cylinder volume due to radial change
ε_{max}	peak strain
$\dot{\varepsilon}$	experimentally imposed strain rate

heart muscle fibers are unlikely to generate or resist force equally in all directions. For example, in mammals, cardiac tissue has been shown to be anisotropic, suggesting that the direction of extension may have functional implications (Demer and Yin, 1983).

In contrast to vertebrate hearts, crustacean hearts are neurogenic, and are controlled directly by the cardiac ganglion (CG), a central pattern generator (CPG) that is embedded in the myocardium (Fig. 1) (Alexandrowicz, 1932; Cooke, 2002). Rhythmic behaviors, such as the neurogenic heartbeat, can be hormonally and locally modulated by neurochemicals, thus generating flexibility in the hard-wired CPG motor output (reviewed in Marder, 1991; Simmers et al., 1995; Pearson, 2000; Hooper and DiCaprio, 2004; Goulding, 2009; Guertin and Steuer, 2009; Brezina, 2010; Christie et al., 2010a; Selverston, 2010).

Although the effects of neuromodulators on crustacean CPG-effector systems are well documented, these studies have only examined the physiological effects at single locations on the length–tension curve (Mercier and Russenes, 1992; Fort et al., 2004; Wilkens et al., 2005; Fort et al., 2007a,b; Stevens et al., 2009; Christie et al., 2010b; Dickinson et al., 2015). However, it is important to consider the functional space in which the neurotransmitters are working. The lobster heart does not work at a single location on its length–tension curve; rather, it functions over a range of lengths. Therefore, it is important to understand how neuromodulators might affect the heart over a range of lengths, and to determine the effects of neuromodulators on active as well as passive length–tension curves. Moreover, neuromodulators might interact with the neuromuscular system differently along various axes. Therefore, a multi-directional analysis of the cardiac length–tension curve can provide a more complete understanding of how the lobster heart generates force, and how that force is altered by neuromodulators.

Thus, this study characterizes the force–length curves for whole lobster hearts subjected to slow lengthening and shortening stretches at constant speeds, both uniaxially and biaxially. Additionally, this study characterizes the same curves in the presence of the neuropeptides SGRN and GYS, in intact (with the CG) and stimulated (without the CG) preparations, to describe how mechanical and physiological properties interact in the cardiac neuromuscular system.

MATERIALS AND METHODS

Animals

Homarus americanus H. Milne-Edwards 1837, weighing 250–450 g, were obtained from local seafood retailers (Brunswick, ME, USA). Lobsters were maintained for up to 3 weeks in recirculating natural seawater aquaria at 10–12°C with a 12 h:12 h light:dark cycle. Lobsters were fed chopped squid weekly. Before dissection, lobsters were packed on ice for 30–45 min.

Chemicals

All experiments were carried out in physiological saline (composition in mmol l^{-1}: 479.12 NaCl, 12.74 KCl, 13.67 $CaCl_2$, 20.00 $MgSO_4$, 3.91 Na_2SO_4, 11.45 Trizma base and 4.82 maleic acid; pH 7.45) maintained at 10–12°C by an in-line Peltier temperature regulator (CL-100 bipolar temperature controller and TCM-1 solution heater/cooler; Warner Instruments, Hamden, CT, USA).

GenScript Corporation (Scotch Plains, NJ, USA) synthesized SGRNFLRFamide (SGRN) and GYSDRNYLRFamide (GYS). The peptides were dissolved in deionized water to make 10^{-3} mol l^{-1}

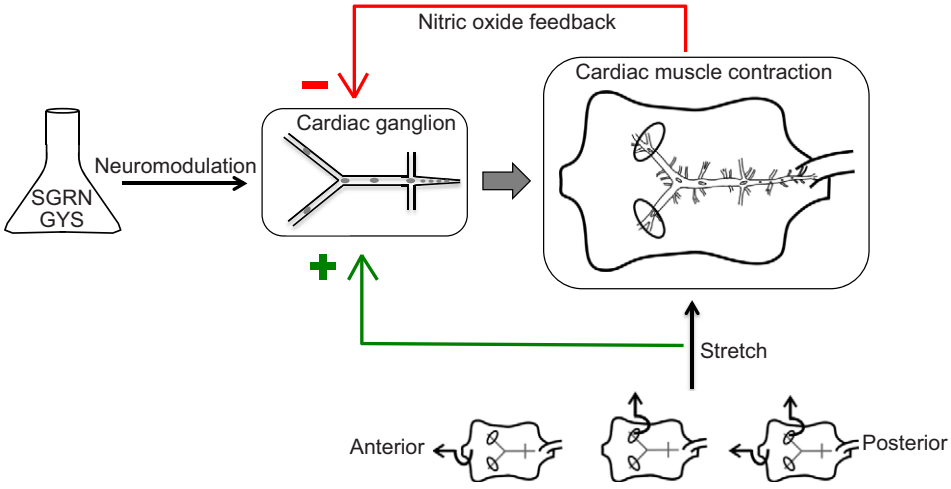

Fig. 1. The lobster cardiac neuromuscular system consists of the cardiac ganglion and its effector tissues. A central pattern generator (CPG) effector system comprises a CPG, effector tissues and feedback pathways. These neural networks can be modulated both intrinsically and extrinsically, thus generating flexibility in the stereotyped output. In addition to modulation by cardioactive neuropeptides, such as SGRNFLRFamide (SGRN) and GYSNRNYLRFamide (GYS), stretch feedback (green) is postulated to modulate cardiac ganglion activity. Nitric oxide generated in the cardiac muscle exerts negative feedback (red). Cartoons illustrate the three types of stretch used in these experiments: longitudinal, transverse and biaxial.

Journal of Experimental Biology

Journal of Experimental Biology (2016) 219, 1187-1202 doi:10.1242/jeb.135657

stock solutions that were stored at −20°C until they were further diluted in physiological saline to the desired concentrations 15–20 min before use. The concentrations of SGRN (10^{-9} mol l^{-1}) and GYS (5×10^{-10} mol l^{-1}) were selected as the lowest concentrations that consistently produced a significant increase in contraction amplitude and frequency (Dickinson et al., 2015).

Whole-heart preparation

The heart, attached to the overlying dorsal carapace, was removed from the lobster. The carapace was pinned in a Sylgard 184 (KR Anderson, Santa Clara, CA, USA)-lined Petri dish filled with chilled physiological saline such that the ventral side of the heart faced upwards. The suspensory ligaments connecting the heart to the carapace were left intact to help preserve the natural stretch required for contraction.

The posterior small artery was cannulated with polyethylene tubing that continuously perfused chilled physiological saline at 2.5 ml min^{-1} and was secured with 6/0 suture silk. A second tube delivered saline to the posterior end of the dish while two outflow tubes were located at the anterior end to facilitate a constant flow of saline across and through the heart. Two Aurora force transducers (Dual-Mode Lever Systems, Model 300C, Aurora Scientific, Aurora, ON, Canada) simultaneously recorded force and imposed stretches on the heart; the sampling rate for force and length was 200 Hz. The signals from the force transducers were amplified by a Model 44 Brownlee Precision Instrumentation amplifier and recorded with a Cambridge Electronic Design (CED) Micro 1401 digitizer paired with Spike2 version 7.03 software (CED, Cambridge, UK). The output of the force transducer is reported in grams rather than Newtons for consistency with other studies that have studied single locations on the length–tension curve (Fort et al., 2004, 2007a,b; Stevens et al., 2009; Christie et al., 2010b; Dickinson et al., 2015).

The levers of the longitudinal and transverse force transducers were attached to the heart via suture silk. The silk was attached at an angle of 90 deg to each lever arm. The longitudinal attachment to the heart was via the five anterior arteries, which were tied together with the suture silk; the transverse attachment to the heart was via a glass hook that was hooked anteriorly through the left ventral ostium. Both force transducers were oriented such that the silk pulled upward at an angle of 30 deg from horizontal; the longitudinal pull on the heart was along the line of the sagittal plane (Fig. 2A). The

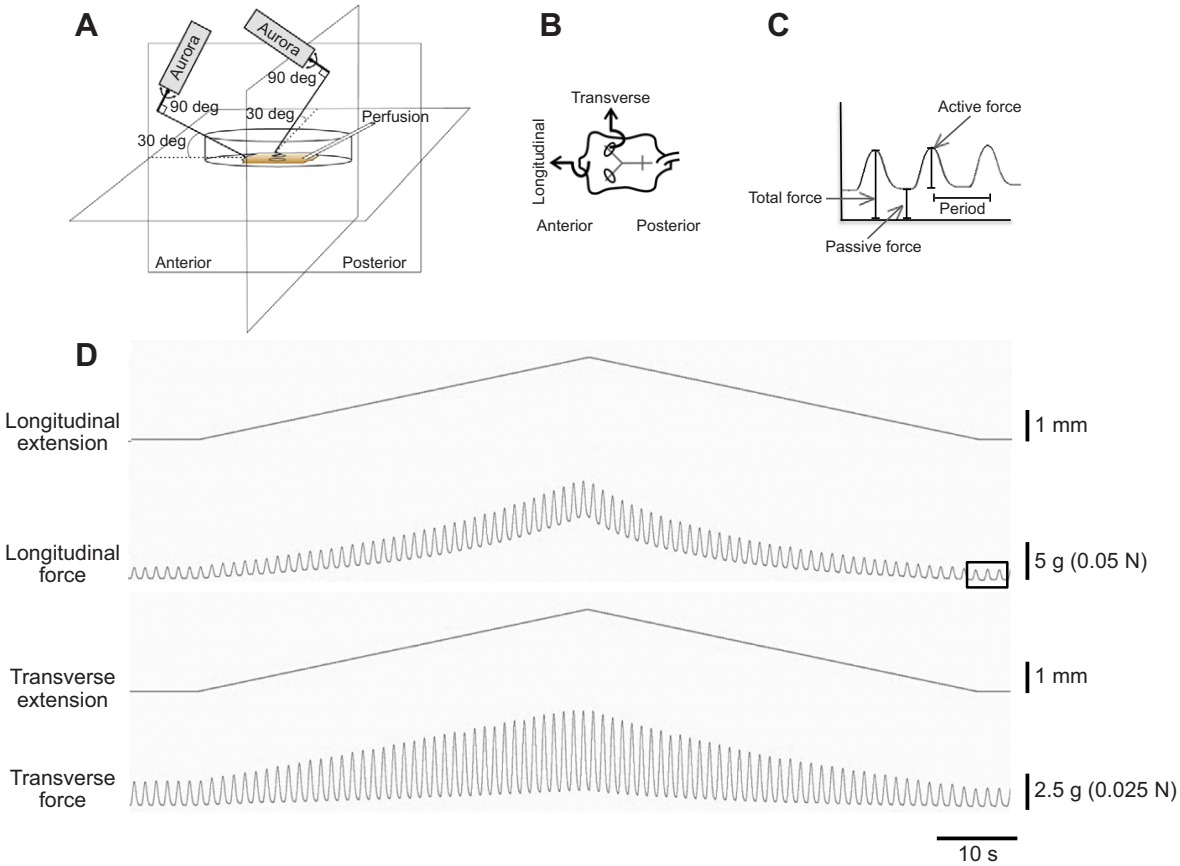

Fig. 2. Schematic diagram of force–extension experiments. Experiments were performed using an Aurora Scientific Dual Mode Lever System (Ontario, Canada). (A) Two force transducers capable of stretching the heart in the longitudinal and transverse directions, respectively, were attached to the heart via suture silk both at an angle of 30 deg from the bottom of the dish. The suture silk was in turn attached to the force transducers at an angle of 90 deg from the line of the lever arm. Peptides and chilled physiological saline were perfused through the heart via the posterior artery. (B) Schematic diagram of the heart, depicting the orientations and direction of the two loading axes. Longitudinal and transverse axes are mutually perpendicular, running along the long and short axes of the heart, respectively. (C) Measurement parameters of the force trace recorded on the Dual Mode Lever System from an enlarged view of the force trace outlined by the square in D. Passive force was quantified when the heart was in the relaxed phase of contraction; active force is the contraction amplitude; total force is the sum of the passive and active forces; period is the time between subsequent contractions; and contraction frequency is the inverse of the period. (D) Example recording of a biaxial stretch pyramid. The heart was stretched simultaneously in both directions, to a maximum extension of 2.17 mm, at a constant extension rate of 0.043 mm s^{-1}.

force–extension relationship for the silk thread is $f=88x^{1.7}$, where f is the force in grams and x is the extension in millimeters (R^2=0.999). Typical maximum forces exerted by the string on the heart range from 2 to 15 g (0.02 to 0.15 N), which correspond to extensions of the silk of 0.11 to 0.35 mm.

Both force transducers were mounted on micromanipulators to allow for fine adjustments in the baseline force. Baseline longitudinal passive force was set at either 1 or 2 g in different experiments. Baseline transverse passive force was set between 0.15 and 0.33 g in each lobster. This lower transverse baseline was used because a transverse baseline greater than 0.5 g resulted in tearing around the ostium in more than 50% of preparations; the lower baseline never caused tears. Thus, all following references to a 1 or 2 g baseline force refer specifically to the longitudinal, baseline passive force. The hearts were stabilized for 1 h at the baseline extensions. Force decreased slightly during the stabilization period; at the end of the stabilization period extensions were manually increased so as to return force to the pre-determined baseline.

Tonic stretch pyramid

Uniaxial and biaxial extension cycles

An Aurora force transducer was used to generate length–tension curves for the lobster heart by imposing a displacement of 2.50 mm at an extension rate of 0.05 mm s^{-1} (50 s extension and 50 s return). To characterize the length–tension curve for the lobster heart, it is essential that the stretch interval be long enough that the interval of a heartbeat is a relatively small fraction of the total stretch, thus necessitating the slow extension rate used in the present study. It is unknown how this extension rate corresponds to *in vivo* strains associated with potential increases in heart filling during periods of higher activity.

Because the Aurora force lever was at a 30 deg angle to the plane of the heart, this displacement of the lever arm resulted in 2.17 mm of displacement of the heart, ΔL_{max}, at a constant extension rate, $\Delta\dot{L}$, of 0.0434 mm s^{-1} along the two major axes of the heart, longitudinal and transverse, while recording the changes in passive, active and total force (Fig. 2). Actual extensions varied slightly because of the compliance of the thread; for example, the average displacement of the connection of the thread to the heart, as measured from the three videos used for strain analysis (see below), was 2.10 mm (±0.13 mm s.d.). To determine the effects of uniaxial extension, stretches were imposed on the heart across one axis, longitudinal or transverse, while extension on the perpendicular axis remained at baseline force; to determine the effects of biaxial extension, stretches were imposed across both axes simultaneously.

Conditioning

Because the heart is a structure composed of viscoelastic materials, and thus experiences stress relaxation, it was conditioned to generate reproducible hysteresis loops within the extension range used in the experiments. Three longitudinal conditioning stretch pyramids were imposed on each heart after an hour-long stabilization at the baseline force. Upon completion of each pyramid, the baseline force, which had experienced slight stress relaxation, was manually returned to either 1 or 2 g of passive force. The heart then recovered for 5 min before the subsequent conditioning pyramid. Using the same protocol, three transverse conditioning stretch pyramids were subsequently imposed on each heart.

Control pyramids

To characterize the control mechanical properties of the heart in saline, three control stretch pyramids were imposed on the heart following the conditioning cycle. Each of the three pyramids (longitudinal, transverse and biaxial), was separated from the previous stretch by a 5-min recovery period. Baseline passive force was readjusted if necessary.

Peptide application

To assess the effects of SGRN (1 and 2 g baseline) and GYS (1 g baseline only) on the force–extension curves, each peptide was applied separately to the same lobster heart.

Following the primary control pyramids, one of the peptides was perfused for 30 min through the heart to allow the effects of the neurotransmitter to stabilize. After the peptide stabilization period, three stretch pyramids (uniaxial longitudinal, uniaxial transverse and biaxial), separated by 5-min recovery periods, were imposed. Immediately after the final stretch pyramid, the peptide was washed from the heart for 1 h with physiological saline; previous work has shown that the effects of GYS and SGRN generally wash out after approximately 20 min (see fig. 1A in Dickinson et al., 2015). Baseline passive force was readjusted if necessary.

The heart was then subjected to a final set of control pyramids (longitudinal, transverse and biaxial) to assess the levels of muscle fatigue or tissue strain. This provided a post-peptide control for the first peptide and, simultaneously, the pre-peptide control for the second peptide. After the control pyramids, the second peptide was applied to the heart using the same procedure as outlined above, including the peptide wash and subsequent set of control stretch pyramids.

Stimulated heart preparation

Neuropeptides, including SGRN and GYS, can exert modulatory effects at several locations within the cardiac neuromuscular system, including the CG and the cardiac muscle or neuromuscular junction (Dickinson et al., 2015). To eliminate effects of the peptides on ganglionic output and record the responses of the periphery (muscle/neuromuscular junction) to peptides, the CG was removed from the whole heart, while the motor nerves remained intact.

The whole heart was prepared as described above until just after the first control stretches in saline. After the first control stretch, a small incision was made on the ventral surface of the heart. The portion of the CG containing the nine neurons was removed. The remaining end of the left anterolateral nerve was gently pulled into a suction electrode. Using stimulation patterns generated in Spike2, the nerve was stimulated in bursts (235 ms, consisting of 15 pulses, each 0.5 ms duration, at 60 Hz) every 1.5 s over 80 s. After the first 15 bursts, a longitudinal uniaxial stretch was imposed on the heart. The group of 15 bursts before the initiation of stretch allowed sufficient time for facilitation (Anderson and Cooke, 1971) and burst-to-burst increases in contraction amplitude during stimulation to stabilize (Stevens et al., 2009). To prevent over-stimulation and nerve damage, the heart was only stimulated during the extension phase of stretch; following completion of the stretch, the heart rested for 5 min without stimulation before a transverse uniaxial stretch was initiated. After the control uniaxial stretches during stimulation, each heart was perfused with either SGRN or GYS for 30 min before longitudinal and transverse uniaxial stretches with stimulation were imposed on the heart. To assess any time-dependent effects, after 1 h of rinsing the peptide from the heart with saline, each heart was stretched uniaxially, in longitudinal and transverse directions, during stimulation.

Strain and strain rate

We videotaped three lobster hearts during each of the three types of stretch (uniaxial along each axis separately and biaxial along both

Journal of Experimental Biology (2016) 219, 1187-1202 doi:10.1242/jeb.135657

axes simultaneously) to quantify peak strain ε_{max} (where L_o is unstretched length) and experimentally imposed strain rate $\dot{\varepsilon}$, imposed by the stretch pyramid:

$$\varepsilon_{max} = \frac{\Delta L_{max}}{L_o}, \quad (1)$$

$$\dot{\varepsilon} = \frac{\varepsilon_{max}}{50\,\text{s}}. \quad (2)$$

An iSight camera (Apple, Cupertino, CA, USA, 1920×1080 pixel resolution, 30 frames s^{-1}), mounted 10 cm above the preparation, recorded the movement of each heart during each type of test stretch pyramid (longitudinal, transverse and biaxial). Carmine particles (Fisher Scientific, Fair Lawn, NJ, USA) sprinkled over the surface of the heart created fixed visual points on the heart. Heart movement was tracked using Tracker Video Analysis and Tracking Tool software (Open Source Physics, www.opensourcephysics.org).

From these videos, we measured longitudinal and transverse L_o and ΔL_{max} and calculated ε_{max} and $\dot{\varepsilon}$. Along both axes, length was measured when the heart was most contracted. Measuring length at a consistent phase of heart contraction was necessary because the compliance in the suture silk attaching the heart to the force transducer allowed the heart to shorten during nearly isometric beats. The nearly isometric beats allowed the heart to shorten by approximately 0.3 mm during each heartbeat as compared with a total lengthening of approximately 2.1 mm during a stretch pyramid. Thus, although the Aurora lever continuously pulled on the end of the silk attached at the lever, the compliance of the suture silk allowed the end of the heart held by the suture silk to shorten with each heartbeat. This effect tends to decrease or increase muscle-shortening rate during the lengthening and shortening phases of the extension cycle, respectively.

Data collection and analyses

Collection and analyses of heart contraction data

Data were analyzed using in-house scripts written for Spike2 that measured the contraction parameters of the heart: amplitude (active force), baseline passive force and peak force (total force) (Fig. 2); data were collected from the onset of the stretch pyramid and for every heartbeat for the subsequent 100 s.

Data were further analyzed using programs written by O. Ellers in Mathematica 9.0.1.0 (Wolfram Research, Champaign, IL, USA). Length–tension curves were generated for the active, passive and total force in each of the lobsters during extension (uniaxial longitudinal, uniaxial transverse and biaxial) in the three treatments (saline, 10^{-9} mol l^{-1} SGRN and 5×10^{-10} mol l^{-1} GYS). Length–tension curves for each lobster heart were generated from interpolated (first order) values of the forces (active, passive and total) during the imposed stretch pyramid from 0.1 to 2.0 mm; using an interpolation avoided assumptions that would have been required in a fitted model. The endpoints (0.0–0.1 mm; 2.0–2.1 mm) were eliminated to reduce extraneous noise caused by contraction occurring during the change in the extension direction. Averaging the interpolated values at 0.1 mm increments generated grouped data curves; the error bars were calculated as the standard error of the interpolated values.

Repeated-measures ANOVA and paired *t*-test analyses

There is significant variation among lobsters; for this reason, all statistical comparisons are paired and thus there are no statistical comparisons between 1 and 2 g longitudinal baseline experiments. All statistical tests are two-tailed.

The variable used for comparison of stretch-dependent changes in passive, active and total forces was the difference between a given force at the highest and lowest extensions, ΔF. The variable called passive force hysteresis was calculated as the area between the extension and return curves of the force versus length graph, divided by the total area under the extension curve calculated relative to the lowest force in the whole curve. Passive force hysteresis represents the passive viscous energy losses during each cycle. For the active force, this calculation represents the difference between active forces generated against a background of lengthening and active forces generated against a background of shortening; for the purposes of parallel language, we call this the active force hysteresis.

For tests conducted without peptides, repeated-measures ANOVA (SPSS version 22.0, IBM, Armonk, NY, USA) were used to compare mean ΔF and hysteresis between test types (uniaxial and biaxial) and measurement axes (longitudinal and transverse), excluding data from the axis perpendicular to the test axis in uniaxial tests.

Paired *t*-tests were used to compare control and neuropeptide results for pre-stretch passive force, pre-stretch active force, $\Delta F_{passive}$, ΔF_{active}, passive force hysteresis and active force hysteresis. For a given peptide treatment, only experiments that included all relevant comparison pairs were included in the analyses.

RESULTS

Peak strains and strain rates

For the three videorecorded hearts, the longitudinal L_o and transverse L_o were, respectively, 2.05 and 1.44 cm, 2.16 and 1.50 cm, and 2.29 and 1.17 cm. Peak strains and strain rates imposed by the stretch pyramid were similar between loading treatments and measurement axes (Fig. 3). The range of strain is similar to the normal physiological strains (0.1) in sarcomeres of the hearts of the crab *Cancer magister* (Meyhöfer, 1993). In videos, the hearts shortened during a heartbeat by an average of 0.28 mm (±0.074 mm s.d., N=36; measured at the start, apex and end of all four stretch pyramids for all three lobster hearts).

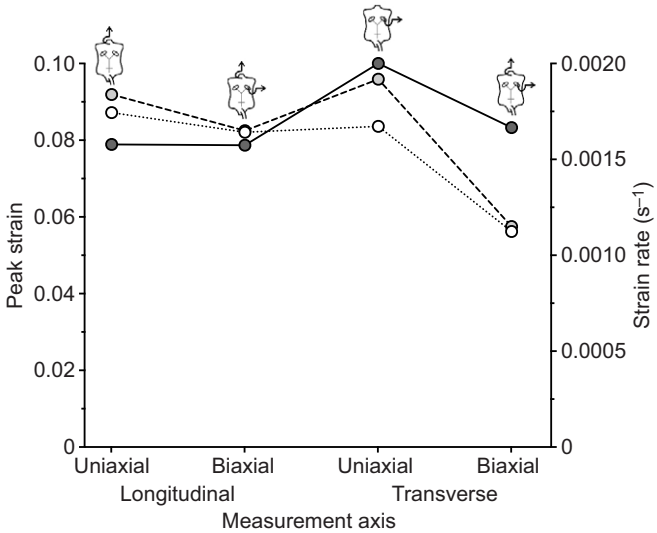

Fig. 3. Peak strains and strain rates were similar between measurement axes. Each fill and line type represents data from one lobster. Peak strains (ε_{max}, left axis) and experimentally imposed strain rates ($\dot{\varepsilon}$, right axis) were similar between loading treatments (uniaxial, biaxial) and measurement axes (longitudinal, transverse).

Journal of Experimental Biology

Journal of Experimental Biology (2016) 219, 1187-1202 doi:10.1242/jeb.135657

Passive, active and total forces increase during stretch

Stretch always elicited an increase in passive, active and total forces along the axis of stretch (Figs 4–6). Passive forces tended to increase in slope with increasing stretch, whereas active forces began to level off above 1.5 mm extension along the longitudinal axis, but increased more steadily along the transverse axis.

Biaxial stretch increased transverse $\Delta F_{passive}$ relative to transverse uniaxial stretch, but biaxial stretch did not affect longitudinal $\Delta F_{passive}$ relative to longitudinal uniaxial stretch. For both biaxial and uniaxial stretches, the increase in $\Delta F_{passive}$ was an order of magnitude greater along the longitudinal than the transverse measurement axis (Fig. 4; see figure legend for statistics).

Biaxial stretch increased ΔF_{active} and ΔF_{total} relative to uniaxial stretch along both measurement axes. When comparing within a given pull type (uniaxial or biaxial), the transverse ΔF_{active} was greater than the longitudinal ΔF_{active} for tests starting from a 1 g baseline, but did not differ between measurement axes for tests starting from a 2 g baseline. Mirroring trends seen in $\Delta F_{passive}$, longitudinal ΔF_{total} was always greater than transverse ΔF_{total} (Figs 5, 6; see legends for statistics).

Passive force hysteresis was greater along the transverse axis whereas active force hysteresis was greater along the longitudinal axis (Figs 5–7; see legend to Fig. 7 for statistics).

GYS and SGRN enhanced some effects of stretch

Although neither peptide altered longitudinal pre-stretch passive force, both peptides significantly increased transverse pre-stretch passive force. Similarly, longitudinal $\Delta F_{passive}$ did not change, or decreased slightly, while transverse $\Delta F_{passive}$ increased in peptide treatments relative to controls, except during biaxial tests in GYS (Fig. 8; see legend for statistics).

Both peptides also significantly increased pre-stretch active force and ΔF_{active} in peptide treatments relative to controls (Fig. 9; see legend for statistics).

Passive force hysteresis decreased with peptide treatment, although the effect of GYS reached significance in only one comparison. Longitudinal active force hysteresis also tended to decrease with peptide treatment; however, transverse active force hysteresis was unaffected by peptides except for one comparison (Figs 8–10; see legend to Fig. 10 for statistics).

Removal of CG input modified the effects of GYS and SGRN

In most cases, neither peptide altered either pre-stretch passive forces or $\Delta F_{passive}$ in stimulated preparations in which the CG was removed. However, similar to intact preparations, SGRN did elicit an increase in the transverse pre-stretch passive force (Fig. 11, see legend for statistics).

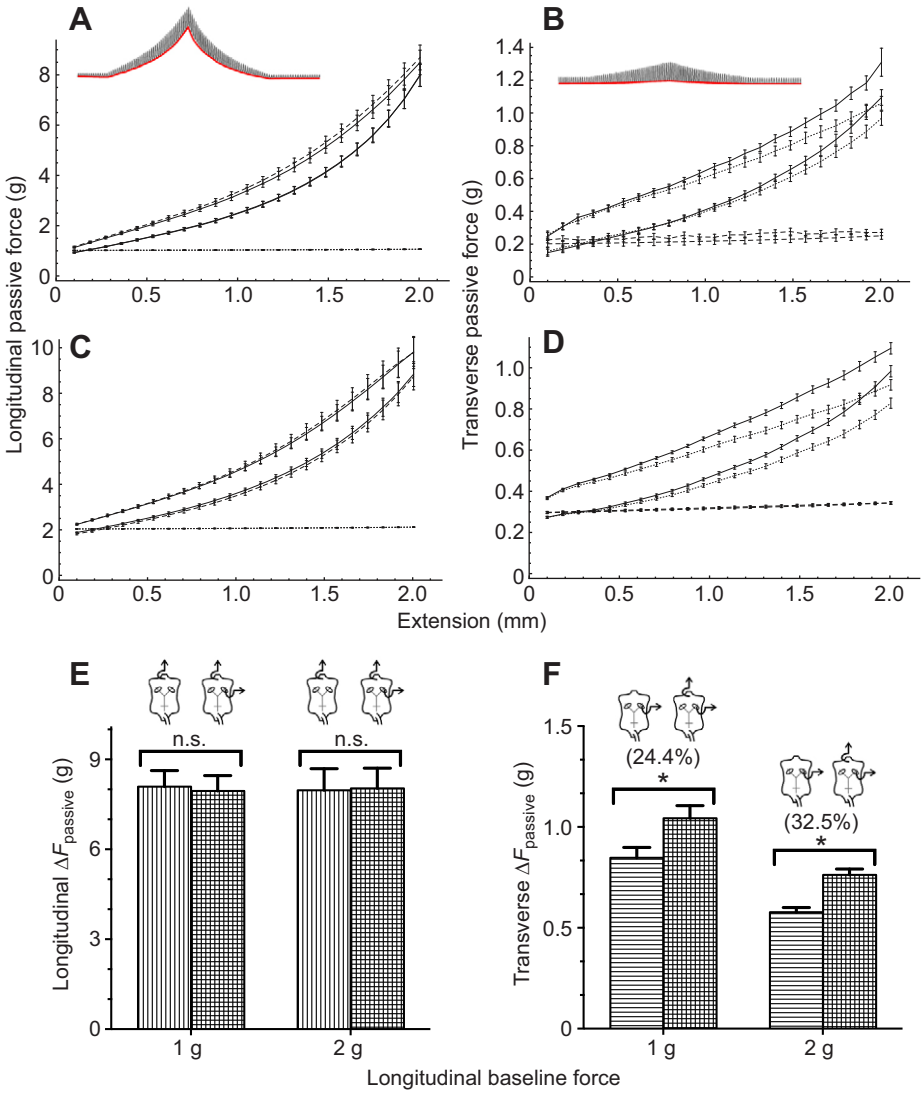

Fig. 4. Passive forces are greater along the longitudinal than the transverse axis in lobster hearts perfused with saline. To one significant figure, force axes values times 10^{-2} are equivalent to N. (A–D) Passive forces (red lines on insets) measured along the longitudinal (A,C) and transverse (B,D) axes during uniaxial longitudinal (dashed lines), uniaxial transverse (dotted lines) and biaxial (solid lines) stretches starting from a 1 g (A,B) and 2 g (C,D) longitudinal baseline passive force. The top line of each line type is the extension phase and the bottom line of each line type is the return phase of each stretch pyramid; thus, stress relaxation occurred during each stretch pyramid. Force increased only minimally, if at all, during uniaxial stretches of the perpendicular axis (bottom force lines on each graph). The error bars represent one standard error of the mean of interpolated (first order) lines. Scales are not shown for insets. (E,F) Stretch-induced changes in passive force ($\Delta F_{passive}$) for trials starting from 1 and 2 g longitudinal baseline passive force as measured along the longitudinal (E) and transverse (F) axes. Vertically lined bars are longitudinal uniaxial pulls, horizontally lined bars are transverse uniaxial pulls and cross-hatched bars are biaxial pulls. Error bars represent one standard error. Asterisks indicate a significant difference between uniaxial and biaxial pulls; the number in parentheses gives the percent difference; 'n.s.' indicates no significant difference between uniaxial and biaxial pulls. The transverse $\Delta F_{passive}$ increased from uniaxial to biaxial loading whereas the longitudinal $\Delta F_{passive}$ did not. The longitudinal $\Delta F_{passive}$ was an order of magnitude greater than the transverse $\Delta F_{passive}$. All statistics are repeated-measures ANOVA (each F>104, P<0.001, N=13 lobsters; LSD *post hoc* tests: each significant at P<0.001, each non-significant at P>0.07).

Journal of Experimental Biology (2016) 219, 1187-1202 doi:10.1242/jeb.135657

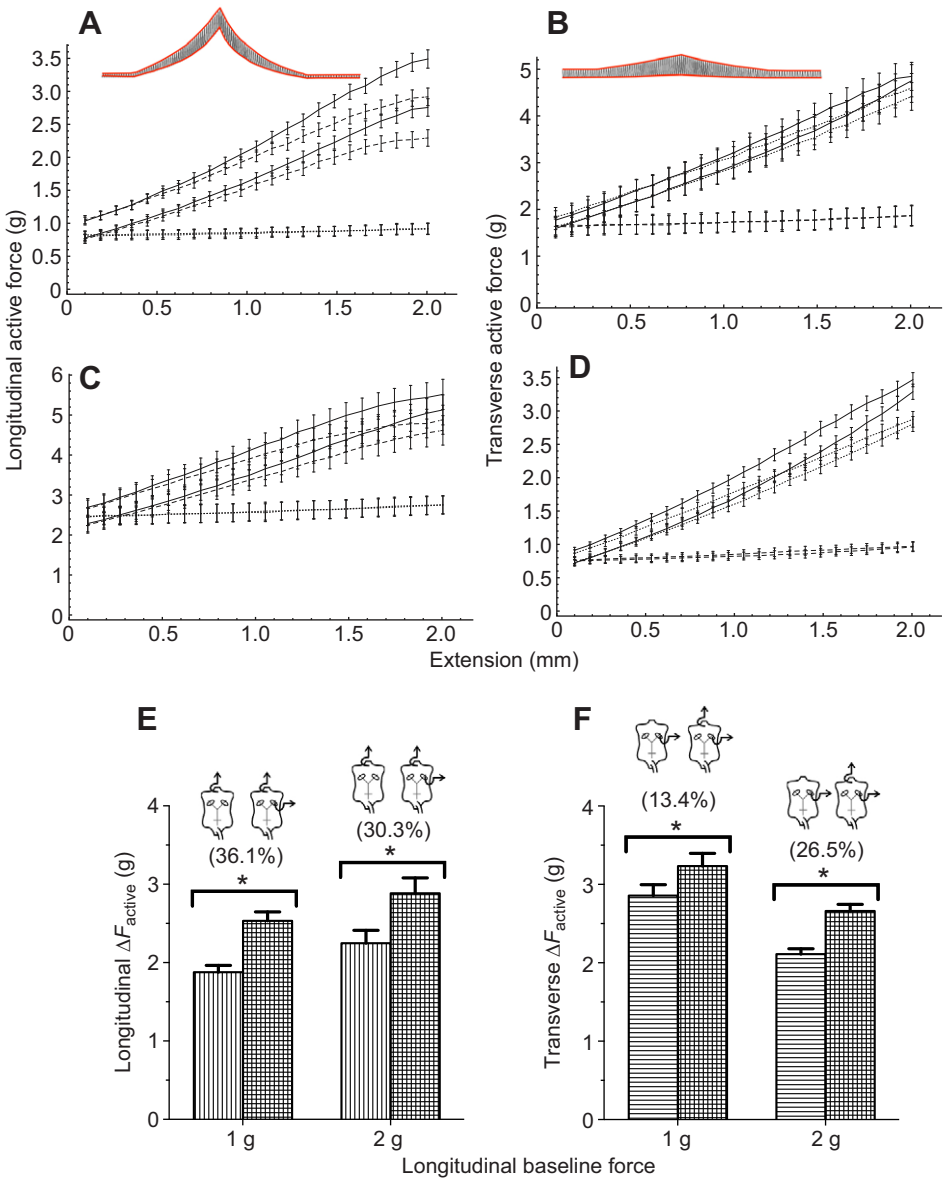

Fig. 5. Biaxial loads increase active forces in lobster hearts perfused with saline. To one significant figure, force axes values times 10^{-2} are equivalent to N. (A–D) Active forces (differences between red lines on insets) measured along the longitudinal (A,C) and transverse (B,D) axes during uniaxial longitudinal (dashed lines), uniaxial transverse (dotted lines) and biaxial (solid lines) stretches starting from a 1 g (A,B) and 2 g (C,D) longitudinal baseline passive force. The top line of each line type is the extension phase and the bottom line of each line type is the return phase of each stretch pyramid. Force increased only minimally, if at all, during uniaxial stretches of the perpendicular axis (bottom force lines on each graph). The error bars represent one standard error of the mean of interpolated (first order) lines. Scales are not shown for insets. (E,F) Stretch-induced changes in active force (ΔF_{active}) for trials starting from 1 and 2 g longitudinal baseline passive force as measured along the longitudinal (E) and transverse (F) axes. Vertically lined bars are longitudinal uniaxial pulls, horizontally lined bars are transverse uniaxial pulls and cross-hatched bars are biaxial pulls. Error bars represent one standard error. Asterisks indicate a significant difference between uniaxial and biaxial pulls; the number in parentheses gives the percent difference. Along both measurement axes, ΔF_{active} increased from uniaxial to biaxial loading. Within a given pull type (uniaxial or biaxial), transverse ΔF_{active} was greater than longitudinal ΔF_{active} for tests starting from a 1 g baseline, but ΔF_{active} did not differ between measurement axes for tests starting from a 2 g baseline. All statistics are repeated-measures ANOVA (each F>9, P<0.01, N=13 lobsters; LSD *post hoc* tests: each significant at P<0.01, each non-significant at P>0.057).

Both peptides caused increases in the pre-stretch active force as well as increases in ΔF_{active} along one measurement axis. Interestingly, longitudinal ΔF_{active} increased in SGRN whereas transverse ΔF_{active} increased in GYS (Fig. 12, see legend for statistics).

DISCUSSION

The lobster heart is anisotropic

Anisotropy in mechanical properties of biological tissues can contribute to tissue-specific functions (Koehl, 1977; Shadwick and Gosline, 1985). For instance, changing the orientation of transverse myofibers in a finite element model of the human left ventricle altered the circumferential–radial shear strains, such that the model matched *in vivo* strains at some orientations (Ubbink et al., 2006). Anisotropy has been measured in canine myocardium, where tissue stiffness was greater under biaxial than uniaxial loads and depended on the direction of extension, with the greatest stiffness aligned with the direction of the predominant fiber (Demer and Yin, 1983). Although anisotropic behavior in myocardium is well characterized in vertebrates (e.g. Yin et al., 1987; Smaill and Hunter, 1991), the present study is the first to characterize whole-heart lobster cardiac length–force curves and to show that the lobster heart is mechanically anisotropic.

Strain, strain rate and anisotropy

One potential contributor to anisotropy is that the heart is approximately 1.4 to 2 times longer than it is wide. Because we applied the same absolute extension to the heart in the longitudinal and transverse directions, this has the potential to exert different strain and strain rates in the longitudinal and transverse directions. Strain rate increases passive muscle stiffness in cardiac myocytes in both vertebrates (Demer and Yin, 1983) and crabs (Meyhöfer, 1993). But our observed strains and strain rates were similar along both axes of stretch (Fig. 3). This occurred because the heart was attached by suture silk on both ends in the longitudinal direction (at the perfusion and at the five anterior arteries) but attached on only one side in the transverse direction (at the hook). Thus, some of the transverse pull resulted in lateral displacement rather than stretch. The observed similarity of strain and strain rates along both axes suggests that passive mechanical differences measured along these

Journal of Experimental Biology (2016) 219, 1187-1202 doi:10.1242/jeb.135657

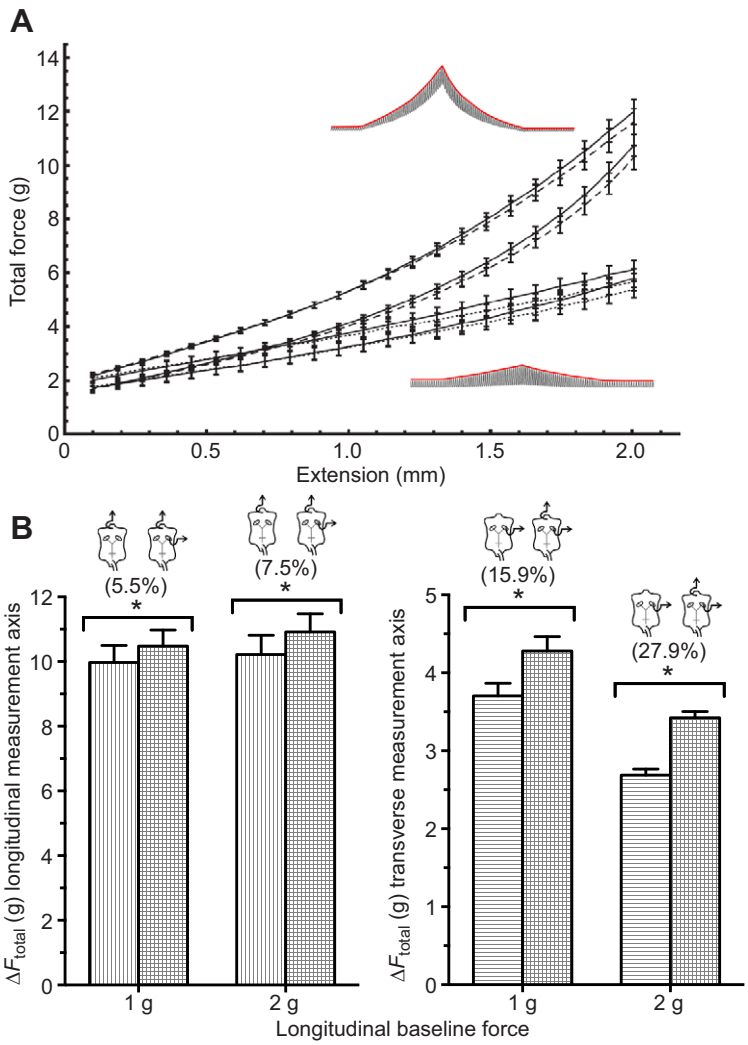

Fig. 6. Total forces are greater along the longitudinal than the transverse axis in lobster hearts perfused with saline. To one significant figure, force axes values times 10^{-2} are equivalent to N. (A) Total force (red lines on insets) measured along the longitudinal axis (upper four lines) and transverse axis (lower four lines) during uniaxial longitudinal (dashed lines), uniaxial transverse (dotted lines) and biaxial (solid lines) stretches starting from a 1 g longitudinal baseline passive force. The top line of each line type is the extension phase and the bottom line of each line type is the return phase of each stretch pyramid, thus, stress relaxation occurred during each stretch pyramid. The total force increased threefold (transverse axis) to sixfold (longitudinal axis). Error bars represent one standard error of the mean of interpolated (first order) lines (N=13 lobsters). Scales are not shown for insets. (B) The change in total force during stretch (ΔF_{total}) for trials starting from 1 and 2 g longitudinal baseline passive force. Vertically lined bars are longitudinal uniaxial pulls, horizontally lined bars are transverse uniaxial pulls and cross-hatched bars are biaxial pulls. Asterisks indicate a significant difference between uniaxial and biaxial pulls; the number in parentheses gives the percent difference. Error bars represent one standard error. ΔF_{total} always increased from uniaxial to biaxial loading. For both 1 and 2 g baselines, longitudinal ΔF_{total} was greater than transverse ΔF_{total}. All statistics are repeated-measures ANOVA (each F>127, P<0.001, N=13 lobsters; LSD *post hoc* tests: each significant at $P \leq 0.001$).

axes represent intrinsic differences in material properties and/or differences in effective material cross-section in the different directions rather than extrinsic differences in strain or strain rate.

Anisotropy in passive forces

Two important contributors to passive force in mammalian myocardium are titin and collagen (Linke et al., 1994, 2002; Granzier and Irving, 1995). Titin contributes more than collagen to passive forces close to slack length because at short sarcomere lengths, collagen is wavy and the passive force necessary to unkink the collagen is low (Hanley et al., 1999; Wu et al., 2000). As sarcomere length increases, collagen straightens and stiffens, such that at the maximal working sarcomere length, collagen contributes as much or more than titin to the passive material properties of cardiac cells (Granzier and Irving, 1995; Hanley et al., 1999; Wu et al., 2000). Because titin tends to have a straighter passive force–extension curve than does collagen, the J-shape of the passive, whole-heart, length–tension curves we observed in lobster heart (Fig. 4) suggests that we might be seeing the effects of collagen at the larger extensions during stretch pyramids. Collagen stiffness may determine end-diastolic volume (Wu et al., 2000); thus the visibility of the J-shape suggests that the lobster's working range may coincide with the range over which we tested.

The low cross-transmission of passive force between the longitudinal and transverse axes of the heart during uniaxial extension (bottom lines in Fig. 4A–D) suggests that muscle or other fibers being pulled are oriented primarily along those axes; greater cross-transmission of force would be expected if obliquely oriented fibers were being loaded. Furthermore, we observed a relatively larger increase in longitudinal passive forces ($\Delta F_{passive}$; Fig. 4, compare E and F); this pattern suggests that the cross-sectional area or stiffness of longitudinal fibers is higher along the longitudinal axis. Locally different mechanical properties within a heart have been observed in bovine atrium versus bovine ventricle due in part to differential expression of titin isoforms of different stiffness (Wu et al., 2000). We also observed higher fractional passive energy losses (hysteresis) along the transverse axis (Fig. 7). Hysteresis is inherently independent of cross-sectional area and high hysteresis is more characteristic of a matrix than a fiber, further suggesting that there is a smaller cross-sectional area of fibers along the transverse axis. However, transverse $\Delta F_{passive}$ was greater during biaxial tests than during uniaxial tests (Fig. 4F) but longitudinal $\Delta F_{passive}$ was not (Fig. 4E), indicating that there is some small cross-transmission of passive force to the transverse axis, but not to the longitudinal axis.

The lobster active length–tension curve

In contrast to passive forces, both longitudinal and transverse ΔF_{active} were significantly higher during biaxial than during uniaxial tests. Higher ΔF_{active} during biaxial tests could be explained if

Journal of Experimental Biology (2016) 219, 1187-1202 doi:10.1242/jeb.135657

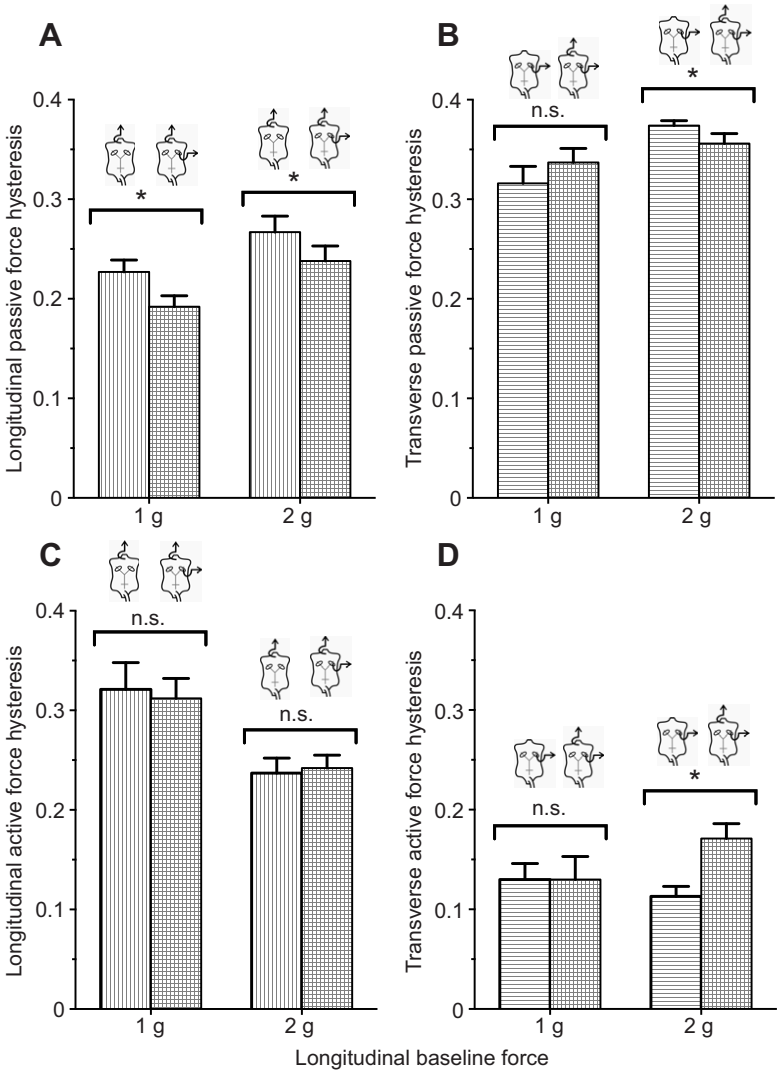

Fig. 7. Passive and active force hysteresis differed between measurement axes. To one significant figure, force axes values times 10^{-2} are equivalent to N. Passive (A,B) and active (C,D) force hysteresis for trials starting from 1 and 2 g longitudinal baseline passive forces as measured along the longitudinal (A,C) and transverse (B,D) axes. Vertically lined bars are longitudinal uniaxial pulls, horizontally lined bars are transverse uniaxial pulls and cross-hatched bars are biaxial pulls. Error bars represent one standard error. Asterisks indicate a significant difference between uniaxial and biaxial pulls. Relative to uniaxial pulls, biaxial pulls tended to decrease passive force hysteresis but increased or did not change active force hysteresis. Transverse passive force hysteresis was greater than longitudinal passive force hysteresis; conversely, transverse active force hysteresis was less than longitudinal active force hysteresis. All statistics are repeated-measures ANOVA (each F>29, P<0.0001, N=13 lobsters; LSD *post hoc* tests: each significant at P<0.02, each non-significant at P>0.1).

muscles were operating at higher sarcomere lengths. For transverse active forces, this explanation is plausible because transverse $\Delta F_{passive}$ values were also higher during biaxial tests, suggesting that the parallel elastic component represented by the passive forces was more stretched. All other things being equal, higher passive forces on the ascending limb correspond to higher sarcomere lengths. But as there were no increases in longitudinal passive forces, the higher active forces observed during biaxial tests invites other explanations. One possibility is that there is stretch feedback such that transverse stretch causes an inotropic increase in active forces in the longitudinal direction.

An increase in active force with extension (Fig. 5A–D) has been observed on the ascending limb of length–tension curves in invertebrate and vertebrate skeletal and cardiac muscle (Brady, 1967; Muhl, 1982; Josephson and Stokes, 1989). Operation on the ascending limb is typically associated with cyclical loading (e.g. hawkmoth wing depressor muscle: Tu and Daniel, 2004; squid mantle muscle: Thompson et al., 2014) and enables larger active forces to be generated at higher extensions. In hearts, the active force increases over the entire working length range, whereas in skeletal muscle, the working range of the active length–tension curve also often includes the descending limb (Burkholder and Lieber, 2001). The continuous increase in active force seen in vertebrate cardiac muscle may be due to: (1) operating only at shorter sarcomere lengths, i.e. on the ascending limb of the length–tension curve; (2) length-dependent sensitivity to calcium; or (3) closer spacing of actin and myosin filaments as length increases, among other possibilities (de Tombe et al., 2010). The length–tension curve of single lobster cardiomyocytes is unknown, but a parabolic-shaped active length–tension curve of a single lobster ostial muscle shows a maximum force at 1.2 times slack length (Yazawa et al., 1999). In comparison, we observed whole-heart length–tension curves that represent 1.1 times baseline length (0.1 strain), where the baseline length is slightly longer than slack length. Thus, assuming similar length–tension curve shapes of ostial and cardio myocytes, the observed whole-heart length–tension curves were likely in the ascending limb. Indeed, although the active length–tension curves are nearly linear, they show a hint of a leveling off at the longer extensions, suggesting that we are reaching the maximum force point on the ascending limb at the highest extensions in our experiment.

Anisotropy in the ratio of passive to active forces

The lobster ostial muscle had a linear passive force–extension curve with a maximum passive force almost 10 times larger than the maximum active force (Yazawa et al., 1999). In the whole lobster heart, we similarly recorded force–extension curves in which passive forces were greater than active forces, but only in the longitudinal direction.

Journal of Experimental Biology (2016) 219, 1187-1202 doi:10.1242/jeb.135657

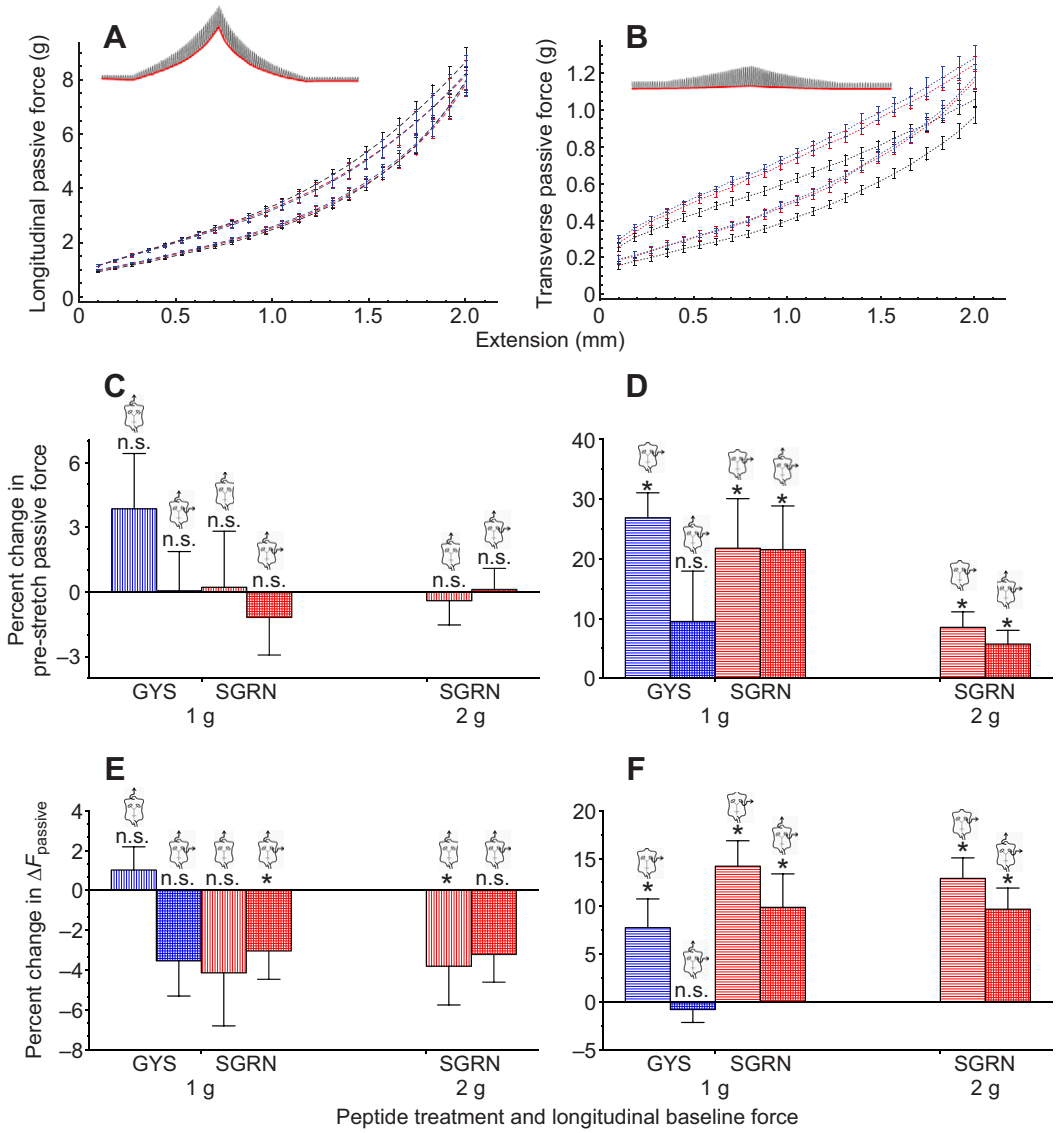

Fig. 8. Passive forces were altered by neuropeptides. To one significant figure, force axes values times 10^{-2} are equivalent to N. (A,B) Passive forces (red lines on insets) for longitudinal and transverse uniaxial pulls measured along the longitudinal (A) and transverse (B) axes, respectively, for lobster hearts perfused with saline (black), SGRN (red) and GYS (blue). The top line of each line color is the extension phase and the bottom line of each line color is the return phase of each stretch pyramid. Error bars represent one standard error of the mean of interpolated (first order) lines. For clarity, data are shown only for stretches started at a longitudinal baseline of 1 g; all experimental data for that baseline are included: *N*=13 controls, 10 SGRN and 7 GYS. Scales are not shown for insets. (C–F) Percent change in pre-stretch passive force (C,D) and $\Delta F_{passive}$ (E,F) relative to saline for trials starting from 1 and 2 g longitudinal baseline forces for lobster hearts perfused with GYS (blue) and SGRN (red) as measured along the longitudinal (C,E) and transverse axes (D,F). Vertically lined bars represent longitudinal uniaxial pulls, horizontally lined bars represent transverse uniaxial pulls and cross-hatched bars represent biaxial pulls. Asterisks indicate a significant difference between control and neuropeptide treatments (paired *t*-tests: each $P<0.035$ for pre-stretch passive force and each $P<0.05$ for $\Delta F_{passive}$); 'n.s.' indicates no significant difference between control and neuropeptide treatments [paired *t*-tests: each $P>0.21$ for pre-stretch passive force and each $P>0.11$ for $\Delta F_{passive}$; GYS *N*=7, SGRN (1 g) *N*=10, SGRN (2 g) *N*=9]. Error bars represent one standard error. Longitudinal pre-stretch passive forces did not change with peptide treatment whereas transverse pre-stretch passive forces increased with peptide treatment. Longitudinal $\Delta F_{passive}$ either decreased or did not change with peptide treatment whereas transverse $\Delta F_{passive}$ increased with peptide treatment. Only data for which there is a complete set of paired data are included.

Active force was less influenced by direction of stretch than was passive force. Because all of the heart muscles contract when the heart is stimulated, differences in force generation must be due either to pre-load differences in fiber or sarcomere length or to differences in inotropy. At the level of the whole heart, differences in active force measured along each axis could also be due to differences in the angle of muscle fibers relative to the axis of measurement. However, because there was little effect of stretch along one axis on active force along the perpendicular axis (flat lines in Fig. 5A–D), we concluded that the fiber angles are unlikely to be important contributors to active force anisotropy. In any case, the active force anisotropy was much less than the passive force anisotropy.

Implications for whole-heart function

Total force did not plateau (Fig. 6) even though the heart approached the length range at which longitudinal active forces did start to plateau. In lobsters, longitudinal and transverse total forces are reaction forces to the forces generated by pressure that is exerted across the heart wall by hemolymph and due to ligaments attaching the heart to external tissues. The total force comprises two

Journal of Experimental Biology

Journal of Experimental Biology (2016) 219, 1187-1202 doi:10.1242/jeb.135657

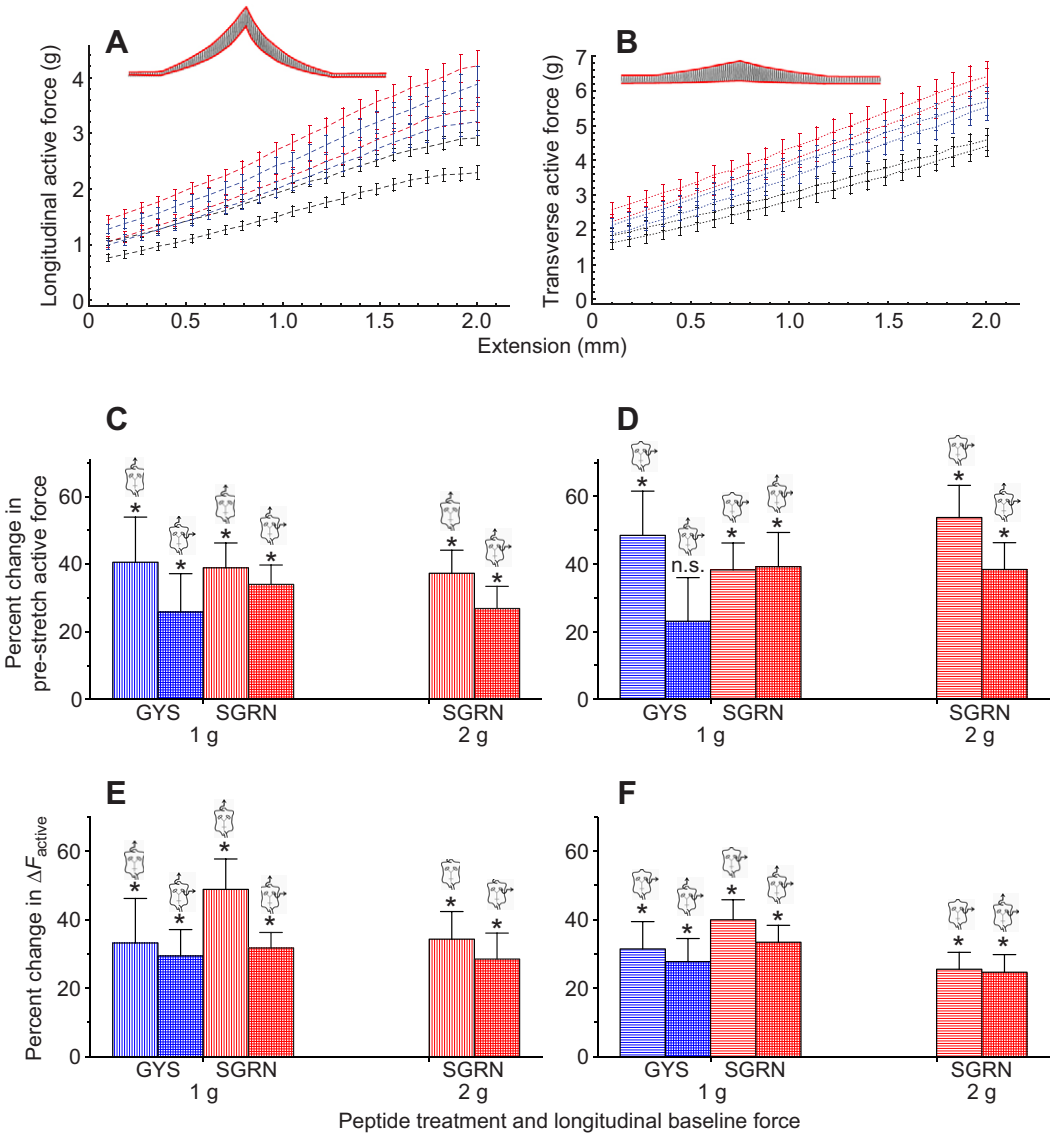

Fig. 9. Active forces increase with neuropeptides. To one significant figure, force axes values times 10^{-2} are equivalent to N. (A,B) Active forces (differences between red lines on insets) for longitudinal and transverse uniaxial pulls measured along the longitudinal (A) and transverse (B) axes, respectively, for lobster hearts perfused with saline (black), SGRN (red) and GYS (blue). The top line of each line color is the extension phase and the bottom line of each line color is the return phase of each stretch pyramid, thus, stress relaxation of active forces occurred during each stretch pyramid along loading axes. The error bars represent one standard error of the mean of interpolated (first order) lines. For clarity, data are shown only for stretches started at a longitudinal baseline passive force of 1 g; all experimental data for that baseline are included: N=13 controls, 10 SGRN and 7 GYS. Scales are not shown for insets. (C–F) Percent change in pre-stretch active force (C,D) and ΔF_{active} (E,F) relative to saline for trials starting from 1 and 2 g longitudinal baseline forces for lobster hearts perfused with GYS (blue) and SGRN (red) as measured along the longitudinal (C,E) and transverse (D,F) axes. Vertically lined bars represent longitudinal uniaxial pulls, horizontally lined bars represent transverse uniaxial pulls and cross-hatched bars represent biaxial pulls. Asterisks indicate a significant difference between control and neuropeptide treatments (paired t-tests, each P<0.05 for pre-stretch active force and P<0.03 for ΔF_{active}); 'n.s.' indicates no significant difference [paired t-test, P>0.18; GYS: N=7, SGRN (1 g): N=10, SGRN (2 g): N=9]. Error bars represent one standard error. Peptides significantly increased pre-stretch active forces and ΔF_{active}. Only data for which there is a complete set of paired data are included.

components: the passive force, which maintains the diastolic wall pressure, and the active force, which produces the heart contraction. Thus, in a beating heart at the longitudinal extensions at which the active force starts to plateau, the longitudinal passive forces increase sharply, resulting in longitudinal total forces that could continue to increase in response to increasing hemolymph pressure within the heart. This combination of forces should enable the heart to pump effectively even at extensions greater than that at which peak active forces are reached.

There are some functional parallels between our mechanical findings for lobster heart and those for octopus aorta. Shadwick and Gosline (1985) found that the octopus aorta exhibits greater passive stiffness along the longitudinal axis than in the circumferential direction. This is similar to the lobster heart, which also has greater longitudinal passive forces. Furthermore, in the octopus aorta, the active forces increase in both longitudinal and transverse directions with increasing extension and are approximately twice as high in the transverse direction as in the longitudinal direction; the same is observed in the lobster heart at the 1 g baseline. Similar to what was observed for the octopus aorta, these anisotropies mean that at a given working pressure, the lobster heart will expand more circumferentially than longitudinally.

Journal of Experimental Biology (2016) 219, 1187-1202 doi:10.1242/jeb.135657

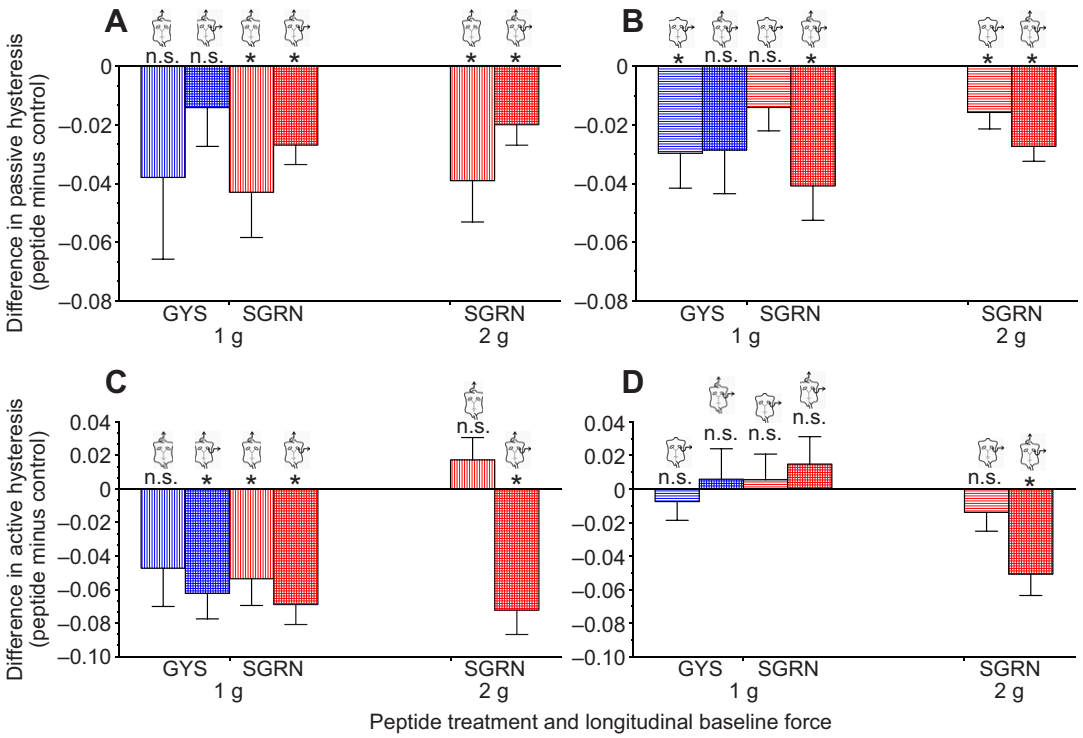

Fig. 10. Passive and active force hysteresis is altered by neuropeptides. To one significant figure, force axes values times 10^{-2} are equivalent to N. Change in passive force (A,B) and active force (C,D) hysteresis for trials starting from 1 and 2 g longitudinal baseline passive forces as measured along the longitudinal (A,C) and transverse (B,D) axes. Vertically lined bars are longitudinal uniaxial pulls, horizontally lined bars are transverse uniaxial pulls and cross-hatched bars are biaxial pulls. Asterisks indicate a significant difference between control and peptide treatments (paired *t*-tests: each $P<0.05$); 'n.s.' indicates no significant difference [paired *t*-tests: each $P>0.08$; GYS (1 g): $N=7$, SGRN (1 g): $N=10$, SGRN (2 g): $N=9$]. Error bars represent one standard error. Passive force hysteresis decreased with SGRN treatment but generally did not significantly decrease with GYS treatment. Longitudinal active force hysteresis decreased with peptide treatment; however, transverse active force hysteresis was generally unaffected by peptide treatment. Only data for which there is a complete set of paired data are included.

Mechanical anisotropy may reflect anisotropy both in how pressure translates into circumferential and longitudinal tension in the walls of the heart and in how circumferential versus longitudinal contractions result in volume changes in the heart. For example, if the heart were shaped as a simple cylinder, then for walls of uniform thickness, pressure would induce twice the hoop stresses relative to the longitudinal stresses in the walls of the heart (Wainwright et al., 1976; Koehl, 1977). However, consider another thought experiment: if the heart is ovoid, with a greater radius of curvature along the longitudinal direction than along the transverse direction, then by LaPlace's law, pressure-induced tension in the wall of the heart would be greater along the longitudinal axis; the greater passive resistance along the longitudinal axis might act to compensate for that added tension. For a cylindrical heart, consider also the consequences of longitudinal or transverse contraction to volume of blood pumped out of the heart during a contraction. For an equivalent strain in the longitudinal and circumferential muscles, a changing radius doubles the volume change relative to a changing length (see Appendix for derivation). Thus, circumferential (and the proportional radial) transverse length changes will be the most significant contributor to the volume of blood pumped.

Neuromodulators exert direct effects on the heart

Active forces can be modulated not only via stretch feedback from the muscles to the CG, but also by the action of neuromodulators acting directly on the CG and/or the periphery. Previous experiments have shown that the effects of the neuropeptides SGRN and GYS differ in experiments on unstretched, intact lobster hearts versus isolated CG (Dickinson et al., 2015). In the present study, we found that both neuropeptides increased pre-stretch active forces not only in intact hearts (Fig. 9C,D), but also in stimulated hearts (Fig. 12C,D), indicating that SGRN and GYS also exert at least some of their effects directly on the heart muscle or neuromuscular junction.

Previous work on lobster hearts has not examined the effect of these neuropeptides on passive forces. We found that neither SGRN nor GYS altered longitudinal pre-stretch passive force (Figs 8C and 11C). Interestingly, both peptides elicited increases (SGRN: 22%; GYS: 27%) in transverse pre-stretch passive forces in intact hearts (Fig. 8D). However, when the CG was removed, GYS no longer caused such an increase, and the rise in passive pre-stretch forces in SGRN was decreased to only 5% (Fig. 11D). These data suggest that much of the increase in passive force is mediated by the CG, perhaps as a result of repeated contractions at higher frequencies (Dickinson et al., 2015), with the consequence that the baseline force does not return to completely relaxed levels, i.e. that some active level of force persists between contractions. However, at least some of the increase seen in the stimulated heart with SGRN is likely a direct effect of the neuropeptide on the muscle because there is some increase in pre-stretch transverse passive force even in the absence of the CG. To our knowledge, this is the first report of a significant effect of neuroactive compounds on passive muscle properties in crustaceans; however, serotonin has been shown to decrease passive muscle tension in leeches (Gerry and Ellerby, 2011; Gerry et al., 2012). Because passive forces at low extensions

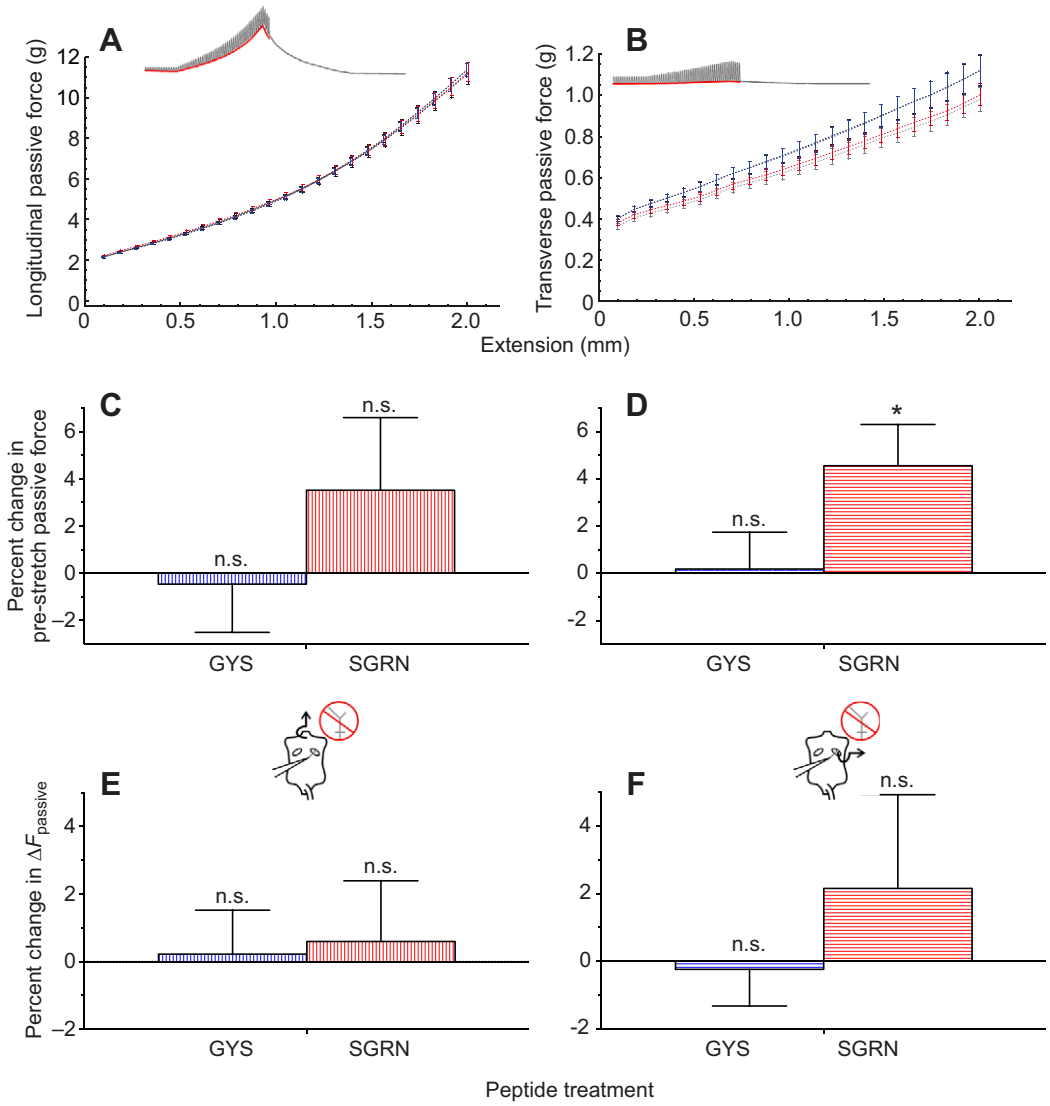

Fig. 11. SGRN elicits an increase in transverse pre-stretch passive force. To one significant figure, force axes values times 10^{-2} are equivalent to N. (A,B) Passive forces (red lines on insets) for longitudinal and transverse uniaxial pulls measured along the longitudinal (A) and transverse (B) axes, respectively, for stimulated lobster hearts perfused with GYS (blue) compared with GYS-control (gray), and SGRN (red) compared with SGRN-control (black). Only the extension phase is shown for each pull. Scales are not shown for insets. Error bars represent one standard error of the mean of interpolated (first order) lines. (C–F) Percent change in pre-stretch passive force (C,D) and $\Delta F_{passive}$ (E,F) relative to saline for lobster hearts perfused with GYS (blue) and SGRN (red) as measured along the longitudinal (C,E) and transverse axes (D,F). Vertically lined bars represent longitudinal uniaxial pulls and horizontally lined bars represent transverse uniaxial pulls. Asterisks indicate a significant difference between control and neuropeptide treatments (paired *t*-tests, each $P<0.03$); 'n.s.' indicates no significant difference (paired *t*-tests, each $P>0.34$ for pre-stretch passive force and $P>0.06$ for $\Delta F_{passive}$; SGRN: $N=10$, GYS: $N=17$). Error bars represent one standard error. SGRN elicited an increase in transverse pre-stretch passive force.

are dominated by titin, perhaps neuropeptides affect titin function in lobster cardiomyocytes. Alternatively, some baseline, non-rhythmic tension could be generated by actin–myosin interactions.

Active and passive hysteresis is reduced by neurotransmitters

Both passive and active forces are lower during the descending ramp than during the ascending ramp of the stretch pyramid. The simplest explanation for this difference for passive forces is that viscoelastic materials always show such hysteresis. But the active force hysteresis requires a different explanation. One possibility is that muscles generate different forces depending on the rate of contraction and the direction of length change. For instance, an eccentrically contracting muscle develops twice as much force as does the same isometrically contracting muscle. And the same concentrically contracting (shortening) muscle develops less force the faster it contracts. Because the pyramids lengthen and shorten the muscle, they will tend to change the eccentric/concentric status of the muscle contraction as well as the velocity of contraction. This is possible because the imposed lengthening speed is much slower than the contraction speed of the heart muscle, and the compliance of the suture silk is such that during the up-ramp, the imposed slow lengthening rate will tend to slightly decrease the shortening velocity of the heartbeat, thus increasing the force slightly relative to the down-ramp. This hypothesized effect is consistent with the observed active force hysteresis (Fig. 7). An alternative explanation is that lengthening of the heart muscle causes different feedback than does shortening and that this feedback alters the force produced. Indeed, neurotransmitters, which might alter feedback, did cause slight decreases in active force hysteresis (Fig. 10C), at

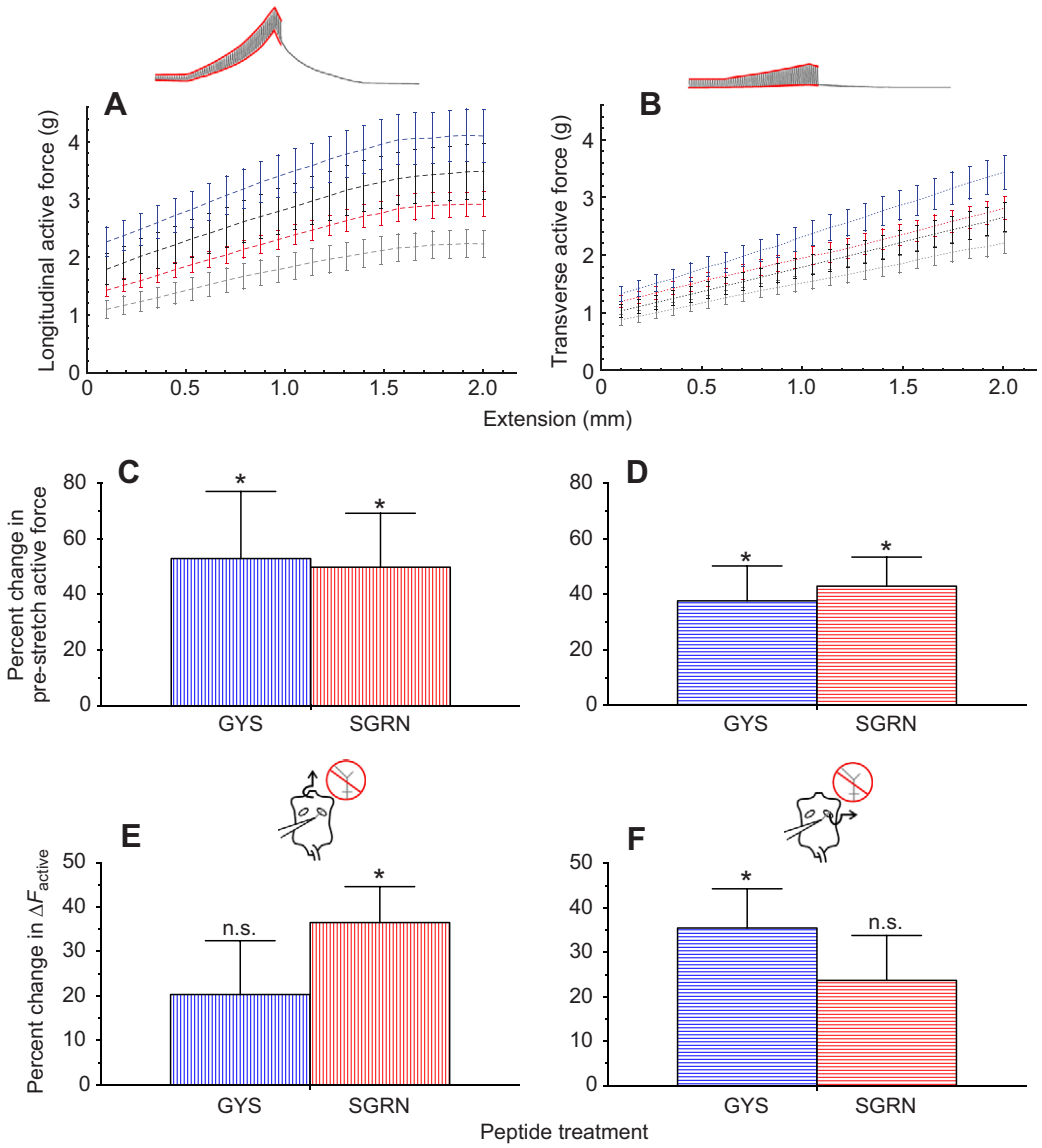

Fig. 12. Active forces increased with neuropeptides. To one significant figure, force axes values times 10^{-2} are equivalent to N. (A,B) Active forces (differences between red lines on insets) for longitudinal and transverse uniaxial pulls measured along the longitudinal (A) and transverse (B) axes, respectively, for stimulated lobster hearts perfused with GYS (blue) compared with GYS-control (gray), and SGRN (red) compared with SGRN-control (black). Only the extension phase is shown for each pull. Scales are not shown for insets. Error bars represent one standard error of the mean of interpolated (first order) lines. (C–F) Percent change in pre-stretch active force (C,D) and ΔF_{active} (E,F) relative to saline for lobster hearts perfused with GYS (blue) and SGRN (red) as measured along the longitudinal (C,E) and transverse axes (D,F). Vertically lined bars represent longitudinal uniaxial pulls and horizontally lined bars represent transverse uniaxial pulls. Asterisks indicate a significant difference between control and neuropeptide treatments (paired *t*-tests, each $P<0.03$ for pre-stretch active force and each $P<0.001$ for ΔF_{active}); n.s. indicates no significant difference (paired *t*-tests, $P_{SGRN}=0.06$ and $P_{GYS}=0.14$ for ΔF_{active}; SGRN: $N=10$, GYS: $N=17$). Error bars represent one standard error. Both peptides increased pre-stretch active forces along both measurement axes, and increased ΔF_{active} along one of the two measurement axes; however, GYS significantly increased transverse ΔF_{active} while SGRN significantly increased longitudinal ΔF_{active}.

least in the longitudinal direction. Additionally, neurotransmitters cause small changes in the passive force hysteresis (Fig. 10A,B), although it is unclear whether this effect on the passive forces is direct or whether it is a result of persistent active forces between heartbeats.

Neuromodulators stiffen the active component of whole-heart length–tension curves

The present study found that these neuromodulators also enhanced the effects of stretch on active forces in both intact and stimulated hearts (Figs 9E,F and 12E,F). One way in which SGRN or GYS might interact with the active length–tension curve is via the combined effects of the initial peptide-induced increase in active force and the stretch-dependent increase in active force, i.e. the neuropeptides shift the curve upwards on the graph. Alternatively, the peptide-induced increase in the slope of active forces as a function of stretch could be the result of stretch feedback from the periphery (Fig. 1). Alexandrowicz (1932) postulated that dendrites with ramifications on the peripheral muscles within the heart might be stretch-sensitive and relay sensory information back to the CG. Thus, the additive effect of stretch and the increased initial contraction force due to the peptides could sufficiently increase the contraction amplitude to trigger the mechanosensitive dendrites, thereby positively regulating the active forces at greater extensions.

Journal of Experimental Biology

One explanation for the apparent multiplicative effects of GYS and SGRN is that both GYS and SGRN increase the duration and frequency, as well as the duty cycle, of cardiac motor neuron bursts (Dickinson et al., 2015), which would result in increased Ca^{2+} availability in cardiac muscles. Given the non-linear nature of the neuromuscular transform (Williams et al., 2013), it is likely that Ca^{2+} also increases non-linearly with stretch. Such a non-linear increase in Ca^{2+} availability, when combined with greater sarcomere lengths, could in turn result in an increase in contraction force that is multiplicative rather than simply additive. Furthermore, the neuropeptides increased ΔF_{active} equally in the longitudinal and transverse directions, supporting the hypothesis that the multiplicative effect was due to the increased availability of actin–myosin interactions at each sarcomere length.

The effect of neuropeptides on ΔF_{active} was maintained in the stimulated preparations (Fig. 12), albeit with some axis-specific differences, further supporting the hypothesis that some of the multiplicative effects of peptides and stretch occur at the neuromuscular junction and/or muscle. Ultimately, the diversity of targets for the neuropeptides enables flexibility in cardiac activity.

The effects of both neuropeptides on stimulated preparations were anisotropic: SGRN only significantly increased longitudinal ΔF_{active} whereas GYS only significantly increased transverse ΔF_{active}. These results suggest that these neuropeptides differ in the location and/or mechanism of action in the muscle or at the neuromuscular junction. Thus, the mechanical anisotropy may be paralleled by a neurophysiological anisotropy. Together, both mechanical and neurophysiological flexibility and anisotropy mediate and control the three-dimensional response of the lobster heart to its environment.

Appendix

For a cylindrical heart, a fractional circumferential contraction causes twice the volume change as does the same fractional length contraction.

For a given fractional length change, $\Delta h/h$, the fractional volume change is:

$$\frac{\Delta v_l}{v} = \frac{\pi r^2 \Delta h}{\pi r^2 h} = \frac{\Delta h}{h}, \quad \text{(A1)}$$

where h is the initial length of the cylinder, v is the initial volume of the cylinder, Δv_l is the change in cylinder volume due to length change and r is the radius of the cylinder.

For a given fractional circumferential change and a proportional fractional radial change, $\Delta r/r_i$, the fractional volume change is:

$$\frac{\Delta v_r}{v} = \frac{\pi h(r_i^2 - r_f^2)}{\pi r_i^2 h} = \frac{(r_i - r_f)(r_i + r_f)}{r_i^2}, \quad \text{(A2)}$$

where Δv_r is the change in cylinder volume due to radial change, and r_i and r_f are the initial and final radii after contraction, respectively. And because $(r_i+r_f)=2r_i+r_f-r_i=2r_i-(r_i-r_f)=2r_i-\Delta r$:

$$\frac{\Delta v_r}{v} = \frac{\Delta r(2r_i - \Delta r)}{r_i^2} = \frac{2\Delta r}{r_i} - \left(\frac{\Delta r}{r_i}\right)^2. \quad \text{(A3)}$$

For small $\Delta r/r_i$:

$$\frac{\Delta v_r}{v} \approx \frac{2\Delta r}{r_i}. \quad \text{(A4)}$$

Therefore, $\Delta v_r \approx 2\Delta v_l$.

Acknowledgements
We thank Hadley Horch, Julie Hewitt and Andrew Calkins for feedback on these experiments, and Marko Melendy for assistance with animal care.

Competing interests
The authors declare no competing or financial interests.

Author contributions
The project was conceived and designed by all four authors. All four authors participated equally in the experimental design and in trouble-shooting the experiments and experimental apparatus. Mathematica programs written by O.E. were used for statistical analyses and figure preparation. E.S.D. performed all experiments. A.S.J. performed the statistical analyses. A.S.J. and E.S.D. created the figures and wrote the drafts of the manuscript. All authors revised the manuscript.

Funding
This research was supported by National Science foundation grant IOS-1121973 and by an Institutional Development Award (IDeA) from the National Institute of General Medical Sciences of the National Institutes of Health under grant number P20GM0103423. The Howard Hughes Medical Institute provided support to E.S.D. via an undergraduate science grant to Bowdoin College. Deposited in PMC for release after 12 months.

References

Alexandrowicz, J. S. (1932). Innervation of the heart of the Crustacea. I. Decapoda. *Quart. J. Microsc. Sci.* **75**, 181-249.
Allen, D. G. and Kentish, J. C. (1985). The cellular basis of the length-tension relation in cardiac muscle. *J. Mol. Cell. Cardiol.* **17**, 821-840.
Anderson, M. and Cooke, I. M. (1971). Neural activation of the heart of the lobster *Homarus americanus*. *J. Exp. Biol.* **55**, 449-468.
Brady, A. J. (1967). Length-tension relations in cardiac muscle. *Am. Zool.* **7**, 603-610.
Brezina, V. (2010). Beyond the wiring diagram: signalling through complex neuromodulator networks. *Philos. Trans. R. Soc. B Biol. Sci.* **365**, 2363-2374.
Burkholder, T. J. and Lieber, R. L. (2001). Sarcomere length operating range of vertebrate muscles during movement. *J. Exp. Biol.* **204**, 1529-1536.
Christie, A. E., Stemmler, E. A. and Dickinson, P. S. (2010a). Crustacean neuropeptides. *Cell. Mol. Life Sci.* **67**, 4135-4169.
Christie, A. E., Stevens, J. S., Bowers, M. R., Chapline, M. C., Jensen, D. A., Schegg, K. M., Goldwaser, J., Kwiatkowski, M. A., Pleasant, T. K., Shoenfeld, L. et al. (2010b). Identification of a calcitonin-like diuretic hormone that functions as an intrinsic modulator of the American lobster, *Homarus americanus*, cardiac neuromuscular system. *J. Exp. Biol.* **213**, 118-127.
Cooke, I. M. (2002). Reliable, responsive pacemaking and pattern generation with minimal cell numbers: the crustacean cardiac ganglion. *Biol. Bull.* **202**, 108-136.
de Tombe, P. P., Mateja, R. D., Tachampa, K., Mou, Y. A., Farman, G. P. and Irving, T. C. (2010). Myofilament length dependent activation. *J. Mol. Cell. Cardiol.* **48**, 851-858.
Demer, L. L. and Yin, F. C. P. (1983). Passive biaxial mechanical properties of isolated canine myocardium. *J. Physiol.* **339**, 615-630.
Dickinson, P. S., Calkins, A. and Stevens, J. S. (2015). Related neuropeptides use different balances of unitary mechanisms to modulate the cardiac neuromuscular system in the American lobster, *Homarus americanus*. *J. Neurophysiol.* **113**, 856-870.
Fort, T. J., Brezina, V. and Miller, M. W. (2004). Modulation of an integrated central pattern generator-effector system: dopaminergic regulation of cardiac activity in the blue crab *Callinectes sapidus*. *J. Neurophysiol.* **92**, 3455-3470.
Fort, T. J., Brezina, V. and Miller, M. W. (2007a). Regulation of the crab heartbeat by FMRFamide-like peptides: multiple interacting effects on center and periphery. *J. Neurophysiol.* **98**, 2887-2902.
Fort, T. J., Garcia-Crescioni, K., Agricola, H.-J., Brezina, V. and Miller, M. W. (2007b). Regulation of the crab heartbeat by crustacean cardioactive peptide (CCAP): central and peripheral actions. *J. Neurophysiol.* **97**, 3407-3420.
Gerry, S. P. and Ellerby, D. J. (2011). Serotonin modulates muscle function in the medicinal leech *Hirudo verbena*. *Biol. Lett.* **7**, 885-888.
Gerry, S. P., Daigle, A. J., Feilich, K. L., Liao, J., Oston, A. L. and Ellerby, D. J. (2012). Serotonin as an integrator of leech behavior and muscle mechanical performance. *Zoology* **115**, 255-260.
Goulding, M. (2009). Circuits controlling vertebrate locomotion: moving in a new direction. *Nat. Rev. Neurosci.* **10**, 507-518.
Granzier, H. L. and Irving, T. C. (1995). Passive tension in cardiac muscle: contribution of collagen, titin, microtubules, and intermediate filaments. *Biophys. J.* **68**, 1027-1044.
Guadagnoli, J. A., Tobita, K. and Reiber, C. L. (2007). Assessment of the pressure-volume relationship of the single ventricle of the grass shrimp, *Palaemonetes pugio*. *J. Exp. Biol.* **210**, 2192-2198.
Guertin, P. A. and Steuer, I. (2009). Key central pattern generators of the spinal cord. *J. Neurosci. Res.* **87**, 2399-2405.

Hanley, P. J., Young, A. A., LeGrice, I. J., Edgar, S. G. and Loiselle, D. S. (1999). 3-Dimensional configuration of perimysial collagen fibres in rat cardiac muscle at resting and extended sarcomere lengths. *J. Physiol.* **517**, 831-837.

Hibberd, M. G. and Jewell, B. R. (1982). Calcium- and length-dependent force production in rat ventricular muscle. *J. Physiol.* **329**, 527-540.

Hooper, S. L. and DiCaprio, R. A. (2004). Crustacean motor pattern generator networks. *Neurosignals* **13**, 50-69.

Josephson, R. K. and Stokes, D. R. (1989). Strain, muscle length and work output in a crab muscle. *J. Exp. Biol.* **145**, 45-61.

Koehl, M. A. R. (1977). Mechanical diversity of connective tissue of the body wall of sea anemones. *J. Exp. Biol.* **69**, 107-125.

Linke, W. A., Popov, V. I. and Pollack, G. H. (1994). Passive and active tension in single cardiac myofibrils. *Biophys. J.* **67**, 782-792.

Linke, W. A., Kulke, M., Li, H., Fujita-Becker, S., Neagoe, C., Manstein, D. J., Gautel, M. and Fernandez, J. M. (2002). PEVK domain of titin: an entropic spring with actin-binding properties. *J. Struct. Biol.* **137**, 194-205.

Marder, E. (1991). Modifiability of pattern generation. *Curr. Opin. Neurobiol.* **1**, 571-576.

Mercier, A. J. and Russenes, R. T. (1992). Modulation of crayfish hearts by FMRFamide-related peptides. *Biol. Bull.* **182**, 333-340.

Meyhöfer, E. (1993). Dynamic mechanical properties of passive single cardiac fibers from the crab *Cancer magister*. *J. Exp. Biol.* **185**, 207-249.

Muhl, Z. F. (1982). Active length-tension relation and the effect of muscle pinnation on fiber lengthening. *J. Morphol.* **173**, 285-292.

Pearson, K. G. (2000). Neural adaptation in the generation of rhythmic behavior. *Annu. Rev. Physiol.* **62**, 723-753.

Selverston, A. I. (2010). Invertebrate central pattern generator circuits. *Philos. Trans. R. Soc. B Biol. Sci.* **365**, 2329-2345.

Shadwick, R. E. and Gosline, J. M. (1985). Mechanical properties of the octopus aorta. *J. Exp. Biol.* **114**, 259-284.

Shiels, H. A. and White, E. (2008). The Frank–Starling mechanism in vertebrate cardiac myocytes. *J. Exp. Biol.* **211**, 2005-2013.

Simmers, J., Meyrand, P. and Moulins, M. (1995). Modulation and dynamic specification of motor rhythm-generating circuits in Crustacea. *J. Physiol. Paris* **89**, 195-208.

Smaill, B. and Hunter, P. (1991). Structure and function of the diastolic heart: material properties of passive myocardium. In *Theory of Heart* (ed. L. Glass, P. Hunter and A. McCulloch), pp. 1-29. New York: Springer.

Stevens, J. S., Cashman, C. R., Smith, C. M., Beale, K. M., Towle, D. W., Christie, A. E. and Dickinson, P. S. (2009). The peptide hormone pQDLDHVFLRFamide (crustacean myosuppressin) modulates the *Homarus americanus* cardiac neuromuscular system at multiple sites. *J. Exp. Biol.* **212**, 3961-3976.

Thompson, J. T., Shelton, R. M. and Kier, W. M. (2014). The length-force behavior and operating length range of squid muscle vary as a function of position in the mantle wall. *J. Exp. Biol.* **217**, 2181-2192.

Tu, M. S. and Daniel, T. L. (2004). Cardiac-like behavior of an insect flight muscle. *J. Exp. Biol.* **207**, 2455-2464.

Ubbink, S. W. J., Bovendeerd, P. H. M., Delhaas, T., Arts, T. and van de Vosse, F. N. (2006). Towards model-based analysis of cardiac MR tagging data: relation between left ventricular shear strain and myofiber orientation. *Med. Image Anal.* **10**, 632-641.

Wainwright, S. A., Biggs, W. D., Currey, J. D. and Gosline, J. M. (1976). *Mechanical Design in Organisms*. New York: John Wiley and Sons.

Wilkens, J. L., Shinozaki, T., Yazawa, T. and ter Keurs, H. E. D. J. (2005). Sites and modes of action of proctolin and the FLP F2 on lobster cardiac muscle. *J. Exp. Biol.* **208**, 737-747.

Williams, A. H., Calkins, A., O'Leary, T., Symonds, R., Marder, E. and Dickinson, P. S. (2013). The neuromuscular transform of the lobster cardiac system explains the opposing effects of a neuromodulator on muscle output. *J. Neurosci.* **33**, 16565-16575.

Wu, Y., Cazorla, O., Labeit, D., Labeit, S. and Granzier, H. (2000). Changes in titin and collagen underlie diastolic stiffness diversity of cardiac muscle. *J. Mol. Cell. Cardiol.* **32**, 2151-2161.

Yazawa, T., Wilkens, J. L., Cavey, M. J., ter Keurs, H. E. D. J. and Cavey, M. J. (1999). Structure and contractile properties of the ostial muscle (musculus orbicularis ostii) in the heart of the American lobster. *J. Comp. Physiol. B Biochem. Syst. Environ. Physiol.* **169**, 529-537.

Yin, F. C. P., Strumpf, R. K., Chew, P. H. and Zeger, S. L. (1987). Quantification of the mechanical properties of noncontracting canine myocardium under simultaneous biaxial loading. *J. Biomech.* **20**, 577-589.